



## A global climatological survey on the ionospheric equivalent slab thickness

Alessio Pignalberi<sup>\*(1)</sup>, Marco Pietrella<sup>(1)</sup>, Bruno Nava<sup>(2)</sup>, Michael Pezzopane<sup>(1)</sup>, Claudio Cesaroni<sup>(1)</sup>,

(1) Istituto Nazionale di Geofisica e Vulcanologia, Rome, Italy

(2) The Abdus Salam International Centre for Theoretical Physics, Trieste, Italy

### Abstract

The main climatological features of the ionospheric equivalent slab thickness ( $\tau$ ) are analyzed on the basis of data collected by three ionospheric stations located at low (Jicamarca, 12.0° S, 76.8° W), mid (Dourbes, 50.1° N, 4.6° E), and high (Thule, 77.5° N, 69.2° W) latitude. F2-layer peak electron density values recorded by ionosondes, and vertical total electron content values from co-located ground-based Global Navigation Satellite System receivers, are used to calculate a dataset of  $\tau$  values for the last two solar cycles, considering only magnetically quiet periods. Results are presented as grids of binned  $\tau$  medians as a function of local time and month of the year, for different solar activity levels. The main climatological features of  $\tau$  are highlighted and discussed, i.e., the diurnal, seasonal, geographic, and solar activity variability.

### 1 Introduction

The ionospheric equivalent slab thickness ( $\tau$ ) is defined as the ratio of the vertical total electron content (vTEC) to the F2-layer peak electron density ( $NmF2$ ) [1]. It is a characteristic parameter of the ionospheric electron density profile representing the equivalent thickness of an ionosphere of uniform electron density equal to  $NmF2$ . Under the same vTEC conditions, small  $\tau$  values are representative of “sharpened” electron density profiles, while high  $\tau$  values are associated to “broadened” profiles. The  $\tau$  behavior is rather complex because it is affected by the simultaneous variability of both the bottomside and the topside ionosphere, and also by important plasmaspheric processes. The main climatological and non-climatological features of  $\tau$  were faced by many authors [2]–[6]. Specifically, the diurnal, seasonal, geographic, solar activity, and magnetic activity variations have been shown to be of great relevance for the  $\tau$  description. However, a reliable description and modeling of  $\tau$  is still a challenge. This summary paper analyses the main climatological features of  $\tau$  at a global scale by exploiting  $NmF2$  values from three ionosonde stations at very different latitudes (Jicamarca, Dourbes, and Thule), and vTEC values from co-located ground-based Global Navigation Satellite System (GNSS) receivers, for a period spanning the last two solar cycles (from 1997 to 2019).

## 2 Data and method

### 2.1 $NmF2$ and vTEC datasets

The  $NmF2$  dataset used in this study consists of data measured during the last two solar cycles (from the

beginning of 1997 to the end of 2019) by the ionosonde stations of Jicamarca, Dourbes, and Thule (Table 1).

Ionosonde (country)	Geographic latitude [°]	Geographic longitude [°]	Years dataset
Dourbes (Belgium)	50.1° N	4.6° E	2004-2019
Jicamarca (Peru)	12.0° S	76.8° W	1997-2018
Thule (Greenland)	77.5° N	69.2° W	2002-2014

**Table 1.** Ionosonde stations with corresponding geographical location and time span covered by datasets.

$NmF2$  values were downloaded from the Digital Ionogram DataBase [7]. For each station, ionograms were recorded by DPS digisondes and autoscaled by the Automatic Real Time Ionogram Scaler with True height analysis (ARTIST) software [8]. ARTIST flags the reliability of autoscaled parameters through the Confidence Score (C-Score) parameter. Only ionograms with C-Score  $\geq 75$  (on a scale from 0 to 100) were selected for this study.  $NmF2$  time series have a fifteen minutes sampling according to the sounding repetition rate of the digisondes at minutes 0, 15, 30, and 45 of each Universal Time (UT) hour.

To calculate  $\tau$  values, we selected GNSS ground-based receivers of the International GNSS Service (IGS, <http://www.igs.org/>) network as near as possible to the ionosonde stations of Table 1, and with a long enough time series of measurements. Table 2 lists the selected GNSS receivers.

GNSS receiver (CODE)	Geographic latitude [°]	Geographic longitude [°]	GNSS receiver network
Redu (REDU)	50.0° N	5.1° E	IGS
Arequipa (AREQ)	16.5° S	71.5° W	IGS
Thule Airbase (THU2)	76.5° N	68.8° W	IGS

**Table 2.** GNSS ground-based receivers co-located with ionosondes of Table 1.

Daily Receiver INdependent EXchange (RINEX) formatted files containing L1 and L2 code and carrier phase data at a 30-seconds sampling time were downloaded from NASA’s GNSS FTP repository (<ftp://cddis.nasa.gov/>). The equivalent vTEC values at the ionospheric pierce point altitude of 350 km were obtained through the Ciralo’s

calibration method [9]. For each GNSS station, at a specific time, a single  $vTEC$  value is obtained from the equivalent  $vTEC$  values calculated for each GPS satellite in view with the cut-off elevation angle set to  $20^\circ$ .  $vTEC$  time series have an original 30-seconds sampling; thus, they need to be uniformed to the  $NmF2$  15-minutes time sampling. This is why,  $vTEC$  values at minutes 0, 15, 30, and 45 of each UT hour were calculated following [10], to obtain 15-minutes weighted mean  $vTEC$  values.

## 2.2 Slab thickness calculation and binning

$\tau$  time series (expressed in meters) were calculated, for each station of Table 1, as the ratio between  $vTEC$  (expressed in  $el/m^2$ ) and  $NmF2$  (expressed in  $el/m^3$ ):

$$\tau = \frac{vTEC}{NmF2}, \quad (1)$$

at a 15-minutes time sampling, when both values were available.

Only magnetically quiet conditions have been studied based on magnetic indices  $Sym-H$  and  $AE$ .  $Sym-H$  index gives information about magnetic disturbances observed on the ground at low and mid latitudes;  $AE$  index instead represents the total intensity of the auroral electrojets and gives information about the disturbance observed at high latitudes due to geomagnetic substorms.  $\tau$  values used in this study are those calculated at the time for which is  $-25 \text{ nT} \leq Sym-H \leq 5 \text{ nT}$  and  $AE \leq 300 \text{ nT}$ .

The solar activity dependence has been studied by binning  $\tau$  time series for three solar activity ranges based on the  $F10.7_{81}$ , i.e., the 81-days running mean of the  $F10.7$  solar index.  $F10.7$  is the solar radio flux at 10.7 cm wavelength (2800 MHz) and represents one of the most used solar activity proxy for ionospheric modeling. In particular, its 81-days running mean has been used in order to smooth its short-time variability to which we are not interested in for this climatological study. The solar activity levels were defined as follows: Low solar activity,  $F10.7_{81} < 80$  s.f.u. (solar flux units,  $1 \text{ s.f.u.} = 10^{-22} \text{ W m}^{-2} \text{ Hz}^{-1}$ ); Medium solar activity,  $80 \text{ s.f.u.} \leq F10.7_{81} < 120$  s.f.u.; High solar activity,  $F10.7_{81} \geq 120$  s.f.u.

Magnetic and solar activity indices were downloaded from OMNIWeb Data Explorer website at [https://spdf.gsfc.nasa.gov/pub/data/omni/high\\_res\\_omni/](https://spdf.gsfc.nasa.gov/pub/data/omni/high_res_omni/). The seasonal dependence of  $\tau$  is studied by binning data for each month of the year (12 bins), while the diurnal dependence is studied by binning data in bins fifteen-minutes wide (96 bins) in local time (LT). So the total number of bins is  $12(\text{month bins}) \times 96(\text{diurnal bins}) = 1152$  for each solar activity level.

For each bin the median value, i.e., the 50<sup>th</sup> percentile, is calculated if at least 10 values are available in the bin. The median is considered the most appropriate statistical quantity when dealing with climatological studies, being less affected by the tails of the distribution (outliers).

## 3 Results and discussion

### 3.1 Low-latitude station: Jicamarca

In Figure 1 the grids of  $\tau$  median values measured at the low-latitude station of Jicamarca, for the three selected

levels of solar activity as a function of LT and month, are presented.

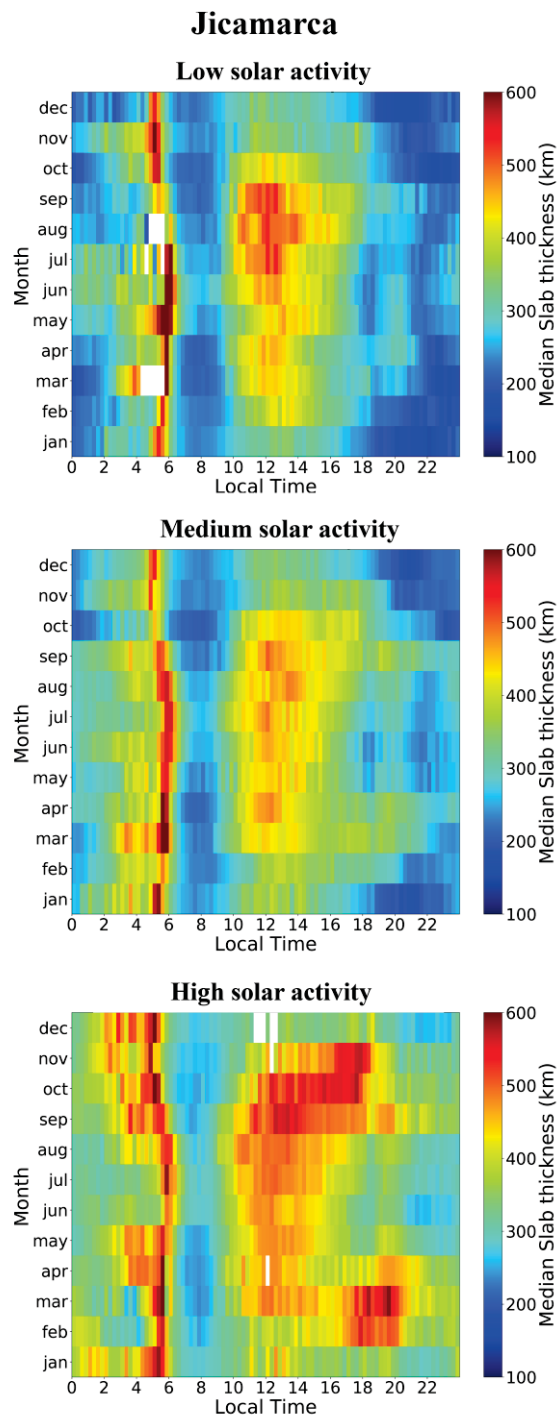


**Figure 1.** Grids of 15-minutes binned medians of equivalent slab thickness measurements at Jicamarca station, for low (top panel), medium (middle panel), and high (bottom panel) solar activity, as a function of local time ( $x$ -axis) and month of the year ( $y$ -axis). Bins with less than 10 values are white colored.

For all solar activity levels,  $\tau$  median values are characterized by two distinct maxima at the morning solar terminator hours and during the central hours of the day. At solar terminator hours, the ionosphere is sunlit differently at different altitudes; then,  $NmF2$  and  $vTEC$  manifest a time

lag which is well reflected in  $\tau$ . For example, at dawn, higher values of  $\tau$  mean that  $NmF2$  is low while  $vTEC$  is increasing due to the solar radiation impinging from above. The reverse is usually observed at dusk hours. Moreover, at low latitudes a morning increase (overshoot) of the electron temperature is observed (usually called pre-sunrise peak) which, being by definition related to the plasma scale height, causes a corresponding increase in  $\tau$  [1]-[3]. The maximum around midday tends to shift to afternoon hours at equinoctial months for high solar activity level. Overall, the lowest  $\tau$  values are observed at night and in the morning hours after dawn. There is an evident seasonal dependence with the highest  $\tau$  values observed for summer and equinoctial seasons; while the lowest values characterize the winter season. This seasonal dependence is related to the solar radiation forcing affecting both  $NmF2$  and  $vTEC$ . A dependence on the solar activity is observed, particularly for high solar activity.

### 3.2 Mid-latitude station: Dourbes

Figure 2 shows the results for the mid-latitude station of Dourbes.

Differently from Jicamarca, Dourbes exhibits the highest values for low solar activity, during the winter night hours. A remarkable seasonal dependence affects the mid latitudes with the highest midday  $\tau$  values observed between the equinoctial months (from March to September), and the lowest ones observed in winter. An evident decrease in  $\tau$  for the dusk hours, the ones characterized by the solar terminator passage, is now very evident for each solar activity level. As previously said, this is due to the time lag characterizing  $NmF2$  and  $vTEC$  at these hours.

### 3.3 High-latitude station: Thule

Figure 3 shows the results for the high-latitude station of Thule.

In this case, a strong solar activity dependence is observed, regardless the season and the hour of the day. Since both  $NmF2$  and  $vTEC$  are mainly affected by the intensity of the solar radiation, a very strong seasonal dependence is observed for the very high-latitude Thule station. For low and medium solar activity, the highest  $\tau$  values are observed for the summer season, for both daytime and nighttime hours, when the solar radiation is always present at such a high latitude. As a consequence, the lowest  $\tau$  values are observed for the winter months when the solar radiation is practically absent there. Differently, the values for high solar activity are less variable with the season. The explanation of this feature needs further studies. Due to the very high latitude, none effect due to the solar terminator passage is observed.

Comparing the three ionospheric stations, it is clear that the behavior of  $\tau$  is strongly dependent on the latitude. This is mainly due to the different behavior that  $NmF2$  and  $vTEC$  exhibit as a function of the solar radiation, which is the first responsible of the observed diurnal and seasonal features. Furthermore, also the influence of the geomagnetic field has to be taken into account because the plasma distribution

in the ionosphere and plasmasphere tends to follow the geometric configuration imposed by the Earth's magnetic field. Then, phenomena specifically connected to the geomagnetic field configuration, like those characterizing the equatorial anomaly and auroral regions, have to be considered to explain some of the observed  $\tau$  features.

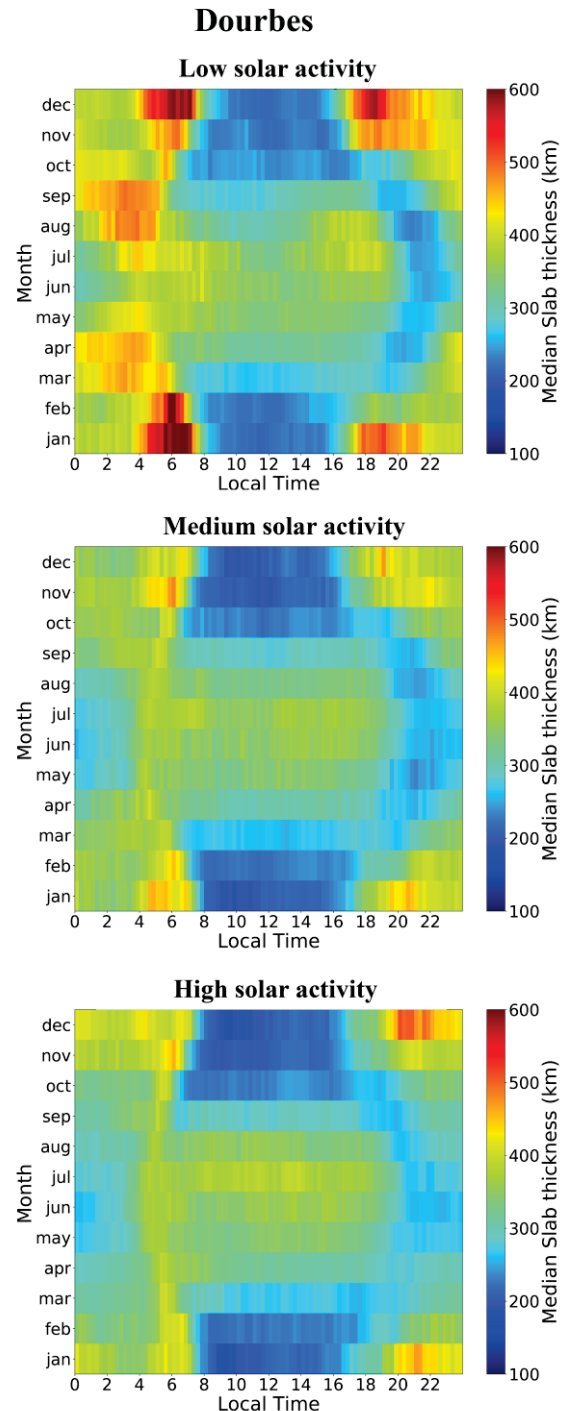
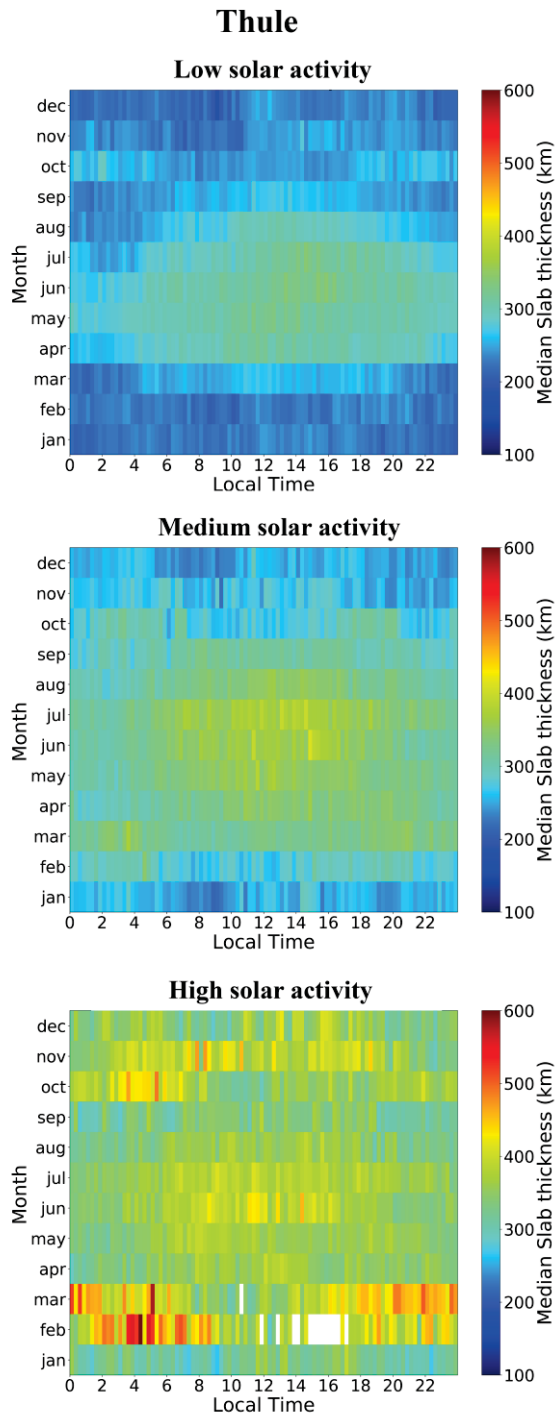


Figure 2. Same as Figure 1 but for Dourbes station.



**Figure 3.** Same as Figure 1 but for Thule station.

## 4 Conclusions

In this study, the climatological behavior of the equivalent slab thickness for different latitudes, and for quiet geomagnetic conditions, has been investigated. The main diurnal, seasonal, geographic, and solar activity features have been described and briefly discussed.

The methodology employed for data selection, filtering, and binning procedures is particularly suited for modeling purposes and constitutes a preliminary step for the implementation of local slab thickness climatological models, that would be really important for a description as

faithful as possible of both the diurnal and seasonal variability of  $\tau$  for different solar activity levels.

## Acknowledgements

This work uses data from ionospheric observatories made available via the public access portal of the Digital Ionogram Database (<http://ulcar.uml.edu/DIDBase/>) of the Global Ionosphere Radio Observatory in Lowell, MA. Thanks to the International GNSS Service (IGS, <http://www.igs.org/>) team for providing and making freely available GNSS data. RINEX files used in this study were downloaded from NASA's GNSS FTP repository (<ftp://cddis.nasa.gov/>). The authors thank Dr. Luigi Ciralo for providing us a tailored version of his vTEC calibration software. Magnetic and solar activity indices used in this study were downloaded from NASA's Space Physics Data Facility of the Goddard Space Flight Center at [https://spdf.gsfc.nasa.gov/pub/data/omni/high\\_res\\_omni/](https://spdf.gsfc.nasa.gov/pub/data/omni/high_res_omni/).

## References

- [1] Titheridge JE (1973) The slab thickness of the mid-latitude ionosphere, *Planetary and Space Science*, 21(10), 1775-1793, [https://doi.org/10.1016/0032-0633\(73\)90168-2](https://doi.org/10.1016/0032-0633(73)90168-2)
- [2] Jayachandran B, Krishnankutty TN, Gulyaeva TL (2004) Climatology of ionospheric slab thickness. *Ann. Geophys.*, 22, 25-33, <https://doi.org/10.5194/angeo-22-25-2004>
- [3] Davies K, Liu XM (1991) Ionospheric slab thickness in middle and low-latitudes. *Radio Sci.* 26 (4), 997-1005, <https://doi.org/10.1029/91RS00831>
- [4] Fox MW, Mendillo M, Klobuchar JA (1991) Ionospheric equivalent slab thickness and its modeling applications. *Radio Sci.*, 26(2), 429- 438, doi:10.1029/90RS02624
- [5] Goodwin GL, Silby JH, Lynn KJW, Breed AM, Essex EA (1995) GPS satellite measurements: ionospheric slab thickness and total electron content. *J. Atmos. Terr. Phys.* 57, 1723-1732, [https://doi.org/10.1016/0021-9169\(95\)00093-H](https://doi.org/10.1016/0021-9169(95)00093-H)
- [6] Stankov SM, Warnant R (2009) Ionospheric slab thickness - analysis, modelling and monitoring. *Adv. Space Res.*, 44, 1295-1303, <https://doi.org/10.1016/j.asr.2009.07.010>
- [7] Reinisch BW, Galkin I (2011) Global Ionospheric Radio Observatory (GIRO). *Earth, Planets and Space*, 63(4), 377-381, <https://doi.org/10.5047/eps.2011.03.001>
- [8] Galkin IA, Reinisch BW (2008) The new ARTIST 5 for all digisondes. *Ionosonde Network Advisory Group Bulletin* 69, <http://www.ips.gov.au/IPSHosted/INAG/web-69/2008/artist5-inag.pdf>
- [9] Ciralo L, Azpilicueta F, Brunini C, Meza A, Radicella SM (2007) Calibration errors on experimental slant total electron content (TEC) determined with GPS. *Journal of Geodesy*, 81(2), 111-120, <https://doi.org/10.1007/s00190 - 006 - 0093 - 1>
- [10] Pignalberi A, Habarulema JB, Pezzopane M, Rizzi R (2019) On the development of a method for updating an empirical climatological ionospheric model by means of assimilated vTEC measurements from a GNSS receiver network. *Space Weather*, 17, 1131-1164, <https://doi.org/10.1029/2019SW002185>